Available online at www.sciencedirect.com
ScienceDirect
Physica A 371 (2006) 25–28
PHYSICA A
www.elsevier.com/locate/physa

Dynamics of an inchworm nano-walker

A. Ciudad[a,*], J.M. Sancho[a], A.M. Lacasta[b]

[a]*Departament d'Estructura i Constituents de la Matèria, Facultat de Física, Universitat de Barcelona, Diagonal 647, E-08028 Barcelona, Spain*
[b]*Departament de Física Aplicada, Universitat Politècnica de Catalunya, Av. Dr. Marañón 44, E-08028 Barcelona, Spain*

Available online 19 May 2006

Abstract

An inchworm processive mechanism is proposed to explain the motion of dimeric molecular motors such as kinesin.We present here preliminary results for this mechanism focusing on observables like mean velocity, coupling ratio and efficiency versus ATP concentration and the external load *F*.

Keywords: Inchworm mechanism; Molecular motor

Molecular motor proteins transform the energy of ATP hydrolysis into mechanical work performing discrete steps along a periodic track. The experimental work on protein motors [1–3] has stimulated a wide variety of modelizations, most of them based in ratchet-like potentials. The two main candidates for the walking mechanisms of dimeric motors were inchworm or hand-over-hand. In the first case it is assumed that the first leading head advances one step which is followed instantaneously by the trailing head. In the hand-over-hand mechanism the second head advances two steps overpassing the first head. In Ref. [2] some experimental evidence was presented which seem to support the inchworm mechanism. Nevertheless, more precise experiments show that myosin-V walk in a hand-over-hand way [3]. These two different mechanisms imply different conformational changes in the protein structure during ATP hydrolysis. Moreover they imply a different response with respect to the experimental control parameters [ATP] and *F*.

Although it is commonly accepted now that some processive members of kinesin, myosin and dynein families seem to walk in a hand-over-hand fashion, it is still worth analyzing the inchworm mechanism, which could hold for other type of motors. For these reasons, we will present here a very simple model walking in a inchworm fashion with parameter values in the biological scale. We will also focus on some implications with experimental relevance.

It was shown in Ref. [1] that kinesin uses a single ATP molecule to perform each step. Such relation is called the coupling ratio, which for low external loads is about 1. The temporal distribution of these steps is random due to the ATP diffusion until it reaches the motor. After binding the nucleotide, hydrolysis and the consequent conformational change take place displacing the whole motor a certain distance which is usually

*Corresponding author.
E-mail addresses: aciudad@ecm.ub.es (A. Ciudad), jmsancho@ecm.ub.es (J.M. Sancho).

0378-4371/$ - see front matter
doi:10.1016/j.physa.2006.04.099

equal to the periodicity of the track. All this process can occur even in the presence of an opposing external force F and at low ATP concentration, although both regimes decrease the mean velocity.

The inchworm walking mechanism can be modeled as two linearly-coupled particles interacting with a ratchet potential. The conformational cycle is introduced as a stretching and posterior relaxing of the coupling spring. This way of modeling was introduced in Ref. [4] showing that thermal fluctuations are not strictly necessary in order to achieve the motion. Other works [5–8] are also based on this approach. The main difference between them is the way they model the mechanical changes under the input of chemical energy. While Ref. [4] considers the conformational change as an increase of the equilibrium length of the spring, other literature introduce asymmetric frictions or switches on the ratchet potential. Here we will explore a different and simple way which allows to control with precision the amount of the input energy. Furthermore, we apply a kinetic methodology [9] based on enzymatic inhibition to get an analytical expression for the velocity as a function of the ATP concentration and the external force F. Finally we analyze the coupling ratio and the efficiency at different values of F.

We will consider the motor as two particles coupled by a spring. The set of equations in the overdamped limit are

$$\lambda\dot{x}_1 = -V'(x_1) - k(x_1 - x_2 - L) - f_s(t) - \frac{F}{2} + \xi_1(t),$$

$$\lambda\dot{x}_2 = -V'(x_2) + k(x_1 - x_2 - L) + f_s(t) - \frac{F}{2} + \xi_2(t), \tag{1}$$

where x_1, x_2 are the position of the trailing and the leading head, respectively, k is the stiffness of the harmonic spring with equilibrium length L, which is also the periodicity of the ratchet potential $V(x)$. Such potential has an asymmetric factor α and a barrier height V_0 (see Fig. 1). $f_s(t)$ is the random chemical force and F is the external load. The thermal force is emulated through a zero mean Gaussian-white noise with a correlation, $\langle\xi_i(t)\xi_i(t')\rangle = 2\lambda k_B T\delta(t - t')$. λ is the friction and $k_B T$ is the thermal energy. Then, at thermal equilibrium the two particles will lay, most of the time, on two consecutive potential minima. We assume that at random intervals of time, an energetic nucleotide like ATP will bind the motor and a stretching force f_s will act on the system until the total length of the motor will be doubled, i.e. $x_2 - x_1 = 2L$. If E is the hydrolysis energy of the molecule and L is the displacement that it is performed, then we take the chemical force $f_s = E/L$.

The values of the parameters have been chosen in a nano scale to mimic some molecular motors such the kinesin. The periodicity of the potential L is taken to be the periodicity of microtubules, 8 nm. The asymmetric factor $\alpha = 0.8$ and $V_0 = 50\,\text{pN nm}$ optimizes the efficiency of our model. $E = 100\,\text{pN nm}$ corresponds to an accepted value for the energy of hydrolysis of an ATP and thermal energy is $k_B T = 4.1\,\text{pN nm}$. The stiffness of the motor is chosen $k = 1\,\text{pN/nm}$ and the drag force $\lambda = 2 \times 10^{-4}\,\text{pNs/nm}$. When the motor is free from

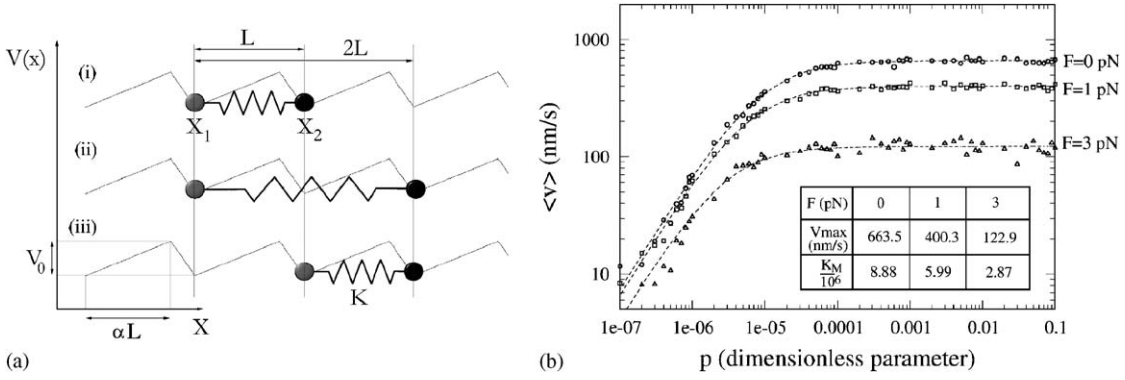

Fig. 1. (a) Scheme of the ratchet potential the positions of the leading head (black particle) and the trailing head (gray particle) at the three stages of the motor. (i) Rest configuration. (ii) The motor at the end of the stretching. (iii) Final stage. (b) Simulated mean velocities $\langle v\rangle$ of the center of mass versus p for $F = 0, 1, 3\,\text{pN}$ drawn with circles, squares and triangles, respectively. Dashed lines are Michaelis–Menten fits. The resulting kinetic parameters are shown in the table.

ATP, $p \in (0,1)$ is the uniform probability per time step Δt of binding one molecule. When it occurs, more ATP binding is forbidden and stretching takes place until the elongation is $2L$. Then, the stretching force disappears and the spring relaxes. When $x_2 - x_1$ is again L, one cycle is completed and ATP binding is allowed. In the absence of external load, this mechano-chemical cycle induces a L displacement of the motor towards one end of the potential. Fig. 1a shows the scheme of the process. On the other hand, our approach controls how much energy E_T is applied to the system by simply multiplying E by the number n of ATP consumed: $E_T = nE$. The mean velocity of the motor, when the ATP concentration is saturant and $F = 0$, is maximum and dependent only on the intrinsic properties of the motor and by E. Let t_{on} be the time spent to perform a single step, i.e., the stretching plus the relaxing time. Thus, $V_{max} = L/t_{on}$. Using the given values of the parameters, simulations show that $t_{on} \sim 0.012\,\mathrm{s}$, which gives $V_{max} \sim 667\,\mathrm{nm/s}$. However, the global speed $\langle v \rangle$ will be slowed down when the ATP concentration decreases. Typically, the $[ATP]$-dependence on $\langle v \rangle$ is given by the Michaelis–Menten relation [9].In our model, we have previously defined p as the uniform probability to get an ATP per time step Δt and with $p = 0$ while the motor stretches and relaxes. It can be accepted that, as the reaction frequency is proportional to $[ATP]$, and then $[ATP]$ is proportional to p. Then, we have

$$\langle v \rangle = V_{max} \frac{p}{K_M + p}, \tag{2}$$

where K_M is the Michaelis constant for the probability. From now on, we will deal with p and not with $[ATP]$. Fig.1b shows how the Michaelian behavior fits well the simulated values of the mean velocity. However, for finite values of F, both kinetic parameters V_{max} and K_M change. In Ref. [9] it is shown that the effect of the external load in kinesin can be interpreted as an inhibition process. This introduces a F-dependence on the two kinetic parameters

$$V_{max}(F) = \frac{V_{max}(F=0)}{1 + 1/K_{iu}(F_S/F - 1)}, \quad K_M(F) = K_M(F=0)\frac{1 + 1/K_{ic}(F_S/F - 1)}{1 + 1/K_{iu}(F_S/F - 1)} \tag{3}$$

and allows to express the velocity of the motor as a function of the two control variables p and F.

F_S is the stall force, i.e., the maximum load that the motor is able to carry. In our simulations, $F_S \sim 5.25\,\mathrm{pN}$. K_{iu} and K_{ic} are the uncompetitive and competitive inhibition constants, respectively, and are a quantitative measure of how F affects the motor when it is free from nucleotide (K_{ic}) or when it has an ATP (K_{iu}). From table values of Fig. 1b we fit the values of the inhibition constants obtaining $K_{iu} \sim 0.338 \times 10^{-6}$ and $K_{ic} \sim 2.131 \times 10^{-6}$. As they are dissociation constants, the effect of the load on the ATP-bound state is greater than in the ATP-free configuration. This means that the force acts as an uncompetitive mixed inhibitor, while in Ref. [9] it is shown that kinesin is also mixed but competitive. This difference is responsible of the curvature on $\langle v \rangle$–F curves at high ATP concentration. Fig. 2a shows these curves with the simulation data and the predictions of the analytical expression with an excellent agreement.

Finally, it is interesting to define the coupling ratio and the efficiency and to see how are they modified by F. The coupling ratio r can be expressed as the quotient between the total number of performed steps and the total number of consumed ATPs. On the other hand, the efficiency η can be defined as the ratio between the work performed against F, W, and the total input of energy, nE. Thus,

$$r \equiv \frac{x_{CM}}{nL}, \quad \eta \equiv \frac{W}{nE}, \tag{4}$$

where $x_{CM} = \frac{1}{2}(x_1 + x_2)$ and supposing that $x_{CM}(t=0) = 0$. $W = F x_{CM}$, so we can write $\eta = rFL/E$. This means that the global efficiency is simply the efficiency in a single step multiplied by the coupling ratio. We can go further if we consider (3) and the fact that V_{max} is proportional to r, and then

$$r = \frac{1}{1 + 1/K_{iu}(F_S/F - 1)}, \quad \eta = \frac{L}{E}\frac{F}{(1 + F/K_{iu}(F_s - F))}. \tag{5}$$

Fig. 2b shows the simulated data for $r(F)$ and $\eta(F)$ as well as the theoretical predictions. It is interesting to remark that the maximum efficiency is slightly below 0.15.

We have presented an inchworm mechanism which is able to perform directed transport and analyzed how it behaves under two variables, the ATP concentration through the probability p and the external load F. The motor can be described as a uncompetitive mixed inhibitor obtaining analytical expressions for the mean

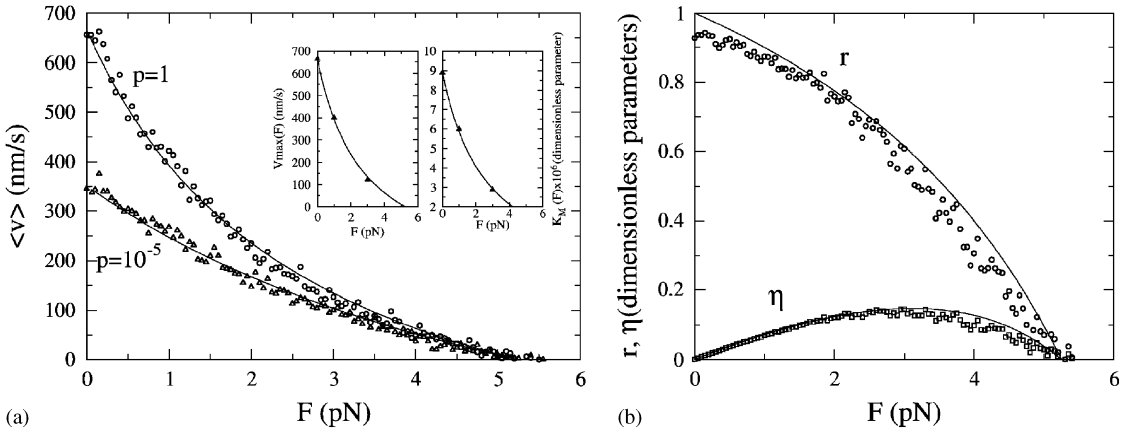

Fig. 2. (a) Simulated mean velocities versus F for $p = 1$ (circles) and $p = 10^{-5}$ (triangles). The insets show $V_{max}(F)$ and $K_M(F)$ versus F. Triangles are the values from the table in Fig. 1b. Solid lines are the fits of (3) in order to get K_{iu} and K_{ic}. With the two inhibition constants, (2) can be plotted obtaining the solid lines of the main figure. (b) Coupling ratio r and efficiency η. Circles are simulated data and solid lines are predictions of (5).

velocity as a function of the two control variables that fits accurately the simulated data. Finally, we have discussed the coupling ratio, showing that the motor loses the tight coupling as F increases. The efficiency is related with the coupling ratio and an analytical expression is given with a good agreement with the simulations.

This work was supported by the Ministerio de Educación y Ciencia (Spain) under the Project no. *BFM*2003-07850 and the Grant no. *BES*-2004-3208(A.C.).

References

[1] K. Visscher, M.J. Schnitzer, S.M. Block, Nature 400 (1999) 184–189.
[2] W. Hua, J. Chung, J. Gelles, Science 295 (2002) 844–848.
[3] C.L. Asbury, A.N. Fehr, S.M. Block, Science 302 (2003) 2130–2134.
[4] G.N. Stratopoulos, T.E. Dialynas, G.P. Tsironis, Phys. Lett. A 252 (1999) 151–156.
[5] D. Dan, A.M. Jayannavar, G.I. Menon, Physica A 318 (2003) 40–47.
[6] H.C. Fogedby, R. Metzler, A. Svane, Phys. Rev. E 70 (2004) 021905.
[7] S. Klumpp, A. Mielke, C. Wald, Phys. Rev. E 63 (2001) 031914.
[8] A. Mogilner, M. Mangel, R.J. Baskin, Phys. Lett. A (1998) 297–306.
[9] A. Ciudad, J.M. Sancho, Biochem. J. 390 (2005) 345–349.